First Measurement of Form Factors of the Decay $\Xi^0 \to \Sigma^+ e^- \overline{\nu}_e$

A. Alavi-Harati,[12] T. Alexopoulos,[12] M. Arenton,[11] K. Arisaka,[2] S. Averitte,[10] R.F. Barbosa,[7,*] A.R. Barker,[5] M. Barrio,[4] L. Bellantoni,[7] A. Bellavance,[9] J. Belz,[10] R. Ben-David,[7] D.R. Bergman,[10] E. Blucher,[4] G.J. Bock,[7] C. Bown,[4] S. Bright,[4] E. Cheu,[1] S. Childress,[7] R. Coleman,[7] M.D. Corcoran,[9] G. Corti,[11] B. Cox,[11] M.B. Crisler,[7] A.R. Erwin,[12] R. Ford,[7] A. Glazov,[4] A. Golossanov,[11] G. Graham,[4] J. Graham,[4] K. Hagan,[11] E. Halkiadakis,[10] J. Hamm,[1] K. Hanagaki,[8] S. Hidaka,[8] Y.B. Hsiung,[7] V. Jejer,[11] D.A. Jensen,[7] R. Kessler,[4] H.G.E. Kobrak,[3] J. LaDue,[5] A. Lath,[10] A. Ledovskoy,[11] P.L. McBride,[7] P. Mikelsons,[5] E. Monnier,[4,†] T. Nakaya,[7] K.S. Nelson,[11] H. Nguyen,[7] V. O'Dell,[7] M. Pang,[7] R. Pordes,[7] V. Prasad,[4] X.R. Qi,[7] B. Quinn,[4] E.J. Ramberg,[7] R.E. Ray,[7] A. Roodman,[4] M. Sadamoto,[8] S. Schnetzer,[10] K. Senyo,[8] P. Shanahan,[7] P.S. Shawhan,[4] J. Shields,[11] W. Slater,[2] N. Solomey,[4] S.V. Somalwar,[10] R.L. Stone,[10] E.C. Swallow,[4,6] S.A. Taegar,[1] R.J. Tesarek,[10] G.B. Thomson,[10] P.A. Toale,[5] A. Tripathi,[2] R. Tschirhart,[7] S.E. Turner,[2] Y.W. Wah,[4] J. Wang,[1] H.B. White,[7] J. Whitmore,[7] B. Winstein,[4] R. Winston,[4,‡] T. Yamanaka,[8] E.D. Zimmerman[4]

(KTeV Collaboration)

[1] *University of Arizona, Tucson, Arizona 85721*
[2] *University of California at Los Angeles, Los Angeles, California 90095*
[3] *University of California at San Diego, La Jolla, California 92093*
[4] *The Enrico Fermi Institute, The University of Chicago, Chicago, Illinois 60637*
[5] *University of Colorado, Boulder, Colorado 80309*
[6] *Elmhurst College, Elmhurst, Illinois 60126*
[7] *Fermi National Accelerator Laboratory, Batavia, Illinois 60510*
[8] *Osaka University, Toyonaka, Osaka 560-0043 Japan*
[9] *Rice University, Houston, Texas 77005*
[10] *Rutgers University, Piscataway, New Jersey 08854*
[11] *The Department of Physics and Institute of Nuclear and Particle Physics, University of Virginia, Charlottesville, Virginia 22901*
[12] *University of Wisconsin, Madison, Wisconsin 53706*

(To be Submited to Physical Review letters, April 11, 2001)

We present the first measurement of the form factor ratios g_1/f_1 (direct axial-vector to vector), g_2/f_1 (second class current) and f_2/f_1 (weak magnetism) for the decay $\Xi^0 \to \Sigma^+ e^- \overline{\nu}_e$ using the KTeV (E799) beam line and detector at Fermilab. From the Σ^+ polarization measured with the decay $\Sigma^+ \to p\,\pi^0$ and the $e^- - \overline{\nu}$ correlation, we measure g_1/f_1 to be $1.32 \pm^{0.21}_{0.17\ \mathrm{stat}} \pm 0.05_{\mathrm{syst}}$, assuming the $SU(3)_f$ values for g_2/f_1 and f_2/f_1. Our results are all consistent with exact $SU(3)_f$ (flavor) symmetry.

PACS numbers: 13.30.Ce, 14.20.Jn

The study of hyperon beta decay plays a fundamental role in discerning the structure of hadrons. The decay $\Xi^0 \to \Sigma^+ e^- \overline{\nu}_e$ is identical to the well measured decay $n \to p\, e^- \overline{\nu}_e$ except that the valence d quarks are replaced by s quarks in the initial and final state baryons. In the limit of exact $SU(3)_f$ (flavor) symmetry the only differences between these processes arise from the different baryon masses and Cabibbo-Kobayashi-Maskawa (CKM) matrix elements. Modifications to the strong interaction dynamics due to the difference between the d and s quark masses can modify the form factors from their $SU(3)_f$ values. Different models for $SU(3)_f$ symmetry breaking, using experimental data from other hyperon beta decays, predict different values for the form factors of the decay $\Xi^0 \to \Sigma^+ e^- \overline{\nu}_e$ [1,2].

The general transition amplitude for the semileptonic decay of a spin 1/2 baryon ($B \to b\, e^- \overline{\nu_e}$) is:

$$\mathcal{M} = G_F V_{CKM} \frac{\sqrt{2}}{2} \overline{u}_b (O^V_\alpha + O^A_\alpha) u_B \times \overline{u_e} \gamma^\alpha (1+\gamma_5) v_\nu + H.c., \quad (1)$$

where

$$O^V_\alpha = f_1 \gamma_\alpha + \frac{f_2}{M_B}\sigma_{\alpha\beta} q^\beta + \frac{f_3}{M_B} q_\alpha,$$
$$O^A_\alpha = (g_1 \gamma_\alpha + \frac{g_2}{M_B}\sigma_{\alpha\beta} q^\beta + \frac{g_3}{M_B} q_\alpha)\gamma_5,$$
$$q^\alpha = (p_e + p_\nu)^\alpha = (p_B - p_b)^\alpha. \quad (2)$$

Here G_F is the Fermi coupling constant, V_{CKM} is the appropriate CKM matrix element, and M_B is the mass of the initial baryon.

When f_3 and g_3 appear in the transition amplitude, they are always multiplied by the electron mass divided by M_B. We therefore neglect them. For $\Xi^0 \to \Sigma^+ e^- \overline{\nu}_e$ the predictions from exact $SU(3)_f$ symmetry (the Cabibbo Model) [3] are: $f_1 = 1.0$, $g_1 = 1.27$ (from $n \to p\, e^- \overline{\nu}_e$), $f_2 = 2.6$, $g_2 = 0$ (no second class current). Deviations from exact $SU(3)_f$ symmetry arising from the differences in the

quark masses can modify the values of the axial-vector form factors [1,2] by up to 20%.

The KTeV (Fermilab E799) experiment reported the first observation [4] of the decay $\Xi^0 \to \Sigma^+ e^- \overline{\nu}_e$. The data presented here were collected during a later four week period of running in 1997 using an improved trigger.

The KTeV neutral beam is produced by an 800 GeV/c proton beam hitting a 30 cm BeO target at an angle of 4.8 mrad. Collimators define two square 0.35 μsr secondary beams. Photons in the beams are converted by a 7.6 cm lead absorber, and charged particles are swept out of the beam by a series of magnets. The sweeping magnets also serve to precess the polarization of the Ξ^0 to the vertical direction. The polarity of the final sweeping magnet is regularly flipped so as to have equal amounts of Ξ^0 polarized in opposite directions, making the ensemble average of the Ξ^0 polarization negligible. An evacuated decay volume extends from 94 m to 159 m downstream of the target. Downstream of the decay volume is a charged particle spectrometer consisting of an analysis magnet and four drift chambers, two upstream and two downstream of the magnet, followed by a CsI electromagnetic calorimeter. The neutral beams pass through two holes in the calorimeter. Other components of the KTeV detector used here are the photon vetoes and the system of transition radiation detectors (TRD). Details of the detector and trigger system can be found elsewhere [4].

The decay chain observed here is $\Xi^0 \to \Sigma^+ e^- \overline{\nu}_e$, with $\Sigma^+ \to p\,\pi^0$ and $\pi^0 \to \gamma\gamma$. The final state consists of five particles: a high momentum proton which travels through one of the calorimeter beam holes, a neutrino which is unobserved, an electron and two photons which are required to hit the calorimeter.

The trigger selects events with a high momentum positively charged track (proton) traveling through one of the beam holes, an opposite charged track (electron) in the CsI calorimeter, and two energy clusters (π^0) not associated with charged tracks.

The decay is reconstructed by finding the longitudinal position of the π^0 decay (z_{π^0}) from the energies and positions of the photon clusters in the calorimeter using the π^0 mass as a constraint. The photon energies are required to be at least 3 GeV and their positions to be at least 1.5 cm away from the edge of either beam hole. The momentum of the π^0 is determined from the extrapolated position of the proton at z_{π^0}. Then the proton and π^0 momenta are added to give the momentum of the Σ^+. Finally, the Σ^+ trajectory is traced back to its closest approach to the electron track, forming the Ξ^0 vertex.

To reduce background from kaon decays, the proton momentum is required to be both between 120 GeV/c and 400 GeV/c and greater than 3.6 times the electron momentum. For electron identification (π^- rejection), we accept only those events in which the energy of the calorimeter cluster associated with the negative track is within 10% of the track momentum. Also, we require a π^- probability of less than 0.1 for the TRD signal associated with the negative track.

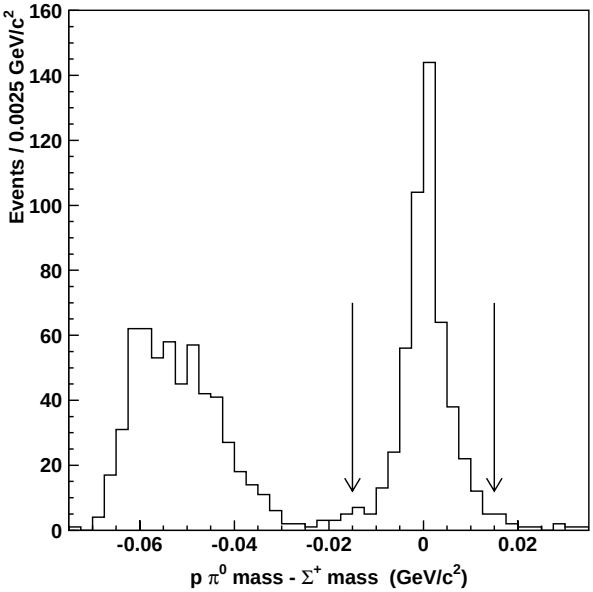

FIG. 1. The $\Sigma^+ \to p\,\pi^0$ mass peak, after all selection criteria have been applied. The background to the left of the peak is due to $\Xi^0 \to \Lambda\,\pi^0$ decays (followed by $\Lambda \to p\,\pi^-$ or $\Lambda \to p e^- \overline{\nu}_e$). Since $\Xi^0 \to \Sigma^+ e^- \overline{\nu}_e$ is the only source of Σ^+ in the beam ($\Xi^0 \to \Sigma^+ \pi^-$ is kinematically forbidden), signal events are identified by having a proton-π^0 mass within 15 MeV/c^2 of the nominal Σ^+ mass.

To remove $K_L \to \pi^0\pi^+ e^- \overline{\nu}$ decays, we require that the $\pi^0\pi^+ e^-$ invariant mass is greater than 0.5 GeV/c^2, or that z_{π^0} is at least 3 m downstream of the Ξ^0 vertex. $K_L \to \pi^+\pi^-\pi^0$ events are suppressed by selecting events with a $\pi^+\pi^-\pi^0$ invariant mass greater than 0.57 GeV/c^2. Photon conversions in the drift chambers upstream of the analyzing magnet are reduced by rejecting events with an extra in-time hit in the horizontal views of these chambers. To reduce background from $K_L \to \pi^+ e^- \overline{\nu}\gamma$, we reject events with an electron track upstream segment projected to the CsI calorimeter within 2 cm of a neutral cluster. For $\Xi^0 \to \Sigma^+ e^- \overline{\nu}_e$ events the Σ^+ vertex is always at or downstream of Ξ^0 vertex within the 1 m measurement error, but for kaon background events there is no relation between the longitudinal positions of the observed false Σ^+ and Ξ^0 vertices. Thus the longitudinal position of the Σ^+ vertex is required to be no more than 6 m upstream of the Ξ^0 vertex, and no more than 40 m downstream of the Ξ^0 vertex.

We calculate the transverse momentum of the Ξ^0 vertex ($\vec{p}_\perp$) by taking the component of the total observed momentum transverse to the line connecting the target to the Ξ^0 vertex. Events where the magnitude of $\vec{p}_\perp$ is larger than the energy of the neutrino in the Ξ^0 frame do not have a physical solution for the neutrino

momentum and are therefore removed.

Signal events are identified by having a proton-π^0 mass within 15 MeV/c^2 of the nominal Σ^+ mass (Fig. 1) [5]. After the application of all selection criteria, we have 494 events in the signal region. We estimate 7.4 ± 3.7 background events under the mass peak. These events are almost entirely due to $K_L \to \pi^+ e^- \overline{\nu} \gamma$ decays with an accidental photon in the detector (3.4 events), and $K_L \to \pi^+ e^- \overline{\nu}$ decays with two accidental photons in the detector (2.0 events). We estimate 0.7 background events come from $\Xi^0 \to \Lambda\, \pi^0$ with $\Lambda \to p\, \pi^-$ and $\pi^0 \to e^+ e^- \gamma$, 0.6 events from $K_L \to \pi^0 \pi^+ e^- \overline{\nu}$, and 0.7 events from other sources.

Since the average Ξ^0 polarization in our data sample is negligible, only four kinematic variables are needed to describe the signal completely. The process $\Xi^0 \to \Sigma^+\, e^-\, \overline{\nu}_e$ can be described by the energy of the electron in the Σ^+ frame and the angle between the electron and neutrino in the Ξ^0 frame. The polarization of the Σ^+ can be described by the angle between the proton and the electron, and the angle between the proton and the neutrino in the Σ^+ frame. The usefulness of the final state polarization is greatly enhanced by the large asymmetry of the decay $\Sigma^+ \to p\, \pi^0$ $(\alpha = -0.98)$.

Since the neutrino is unobserved, we cannot unambiguously reconstruct the directions in the center of mass. However, assuming the observed $\vec{p}_\perp$ is equal and opposite to the transverse momentum of the neutrino, we can obtain unambiguous angular variables transverse to the direction of the Ξ^0 momentum. Following Dworkin [6], we consider the decay sequence

$$\Xi^0 \ \to Q + \overline{\nu_e}\,, \ \ Q \to \Sigma^+ \ + e^- \qquad (3)$$

where we have introduced the fictitious particle Q. We then construct angular variables out of these transverse quantities. Denoting quantities in the Q rest frame with an asterisk, we have the transverse momenta of the electron, proton, and neutrino in the Q frame: $\vec{p}^{\,*}_{e\perp}$, $\vec{p}^{\,*}_{p\perp}$ and $\vec{p}^{\,*}_{\nu\perp}$ which is approximately equal to $\vec{p}_{\nu\perp}$ since the Ξ^0 and Q momenta are nearly parallel.

The magnitudes of the momenta in the Q frame are calculated to obtain the unambiguous kinematic quantities:

$$x_{p\nu\perp} = \frac{\vec{p}^{\,*}_{p\perp} \cdot \vec{p}_{\nu\perp}}{|\,\vec{p}^{\,*}_{p}\,|\; {E_\nu}^*} \quad \text{and} \quad x_{e\nu\perp} = \frac{\vec{p}^{\,*}_{e\perp} \cdot \vec{p}_{\nu\perp}}{{E_e}^* {E_\nu}^*} \qquad (4)$$

which correspond to the polarization of the Σ^+ along the neutrino direction, and the electron-neutrino correlations, respectively. The kinematic quantity corresponding to the proton-electron correlation is x_{pe}, the cosine of the angle between the proton and the electron in the Σ^+ frame. The one dimensional distributions for x_{pe}, $x_{e\nu\perp}$ and $x_{p\nu\perp}$ are shown in Fig 2.

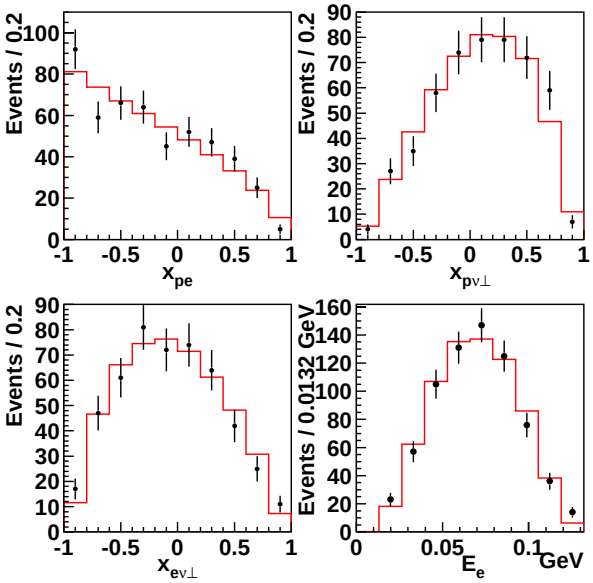

FIG. 2. The three variables used to fit g_1/f_1 and g_2/f_1, and the energy spectrum of the electron in the Σ^+ frame (used to determine f_2/f_1). The points are data and the histogram is our Monte Carlo simulation with $g_1/f_1 = 1.27$ and $g_2/f_1 = 0$.

To determine g_1/f_1, rather than calculate the asymmetries individually, we perform a maximum likelihood fit for g_1/f_1 using x_{pe}, $x_{p\nu\perp}$ and $x_{e\nu\perp}$. We create a $10 \times 10 \times 10$ histogram for data, and create corresponding histograms for different Monte Carlo (MC) values of g_1/f_1. Simulated events are reconstructed in the same manner as data events, and different MC values of g_1/f_1 are obtained by re-weighting the reconstructed MC events according to the differential decay rate [7,8] using the *generated* MC kinematic variables. We then calculate the log likelihood for each g_1/f_1. The central value is the value of g_1/f_1 which maximizes the total log likelihood ($\mathcal{L}$), with the standard errors being determined by change in g_1/f_1 which changes $\mathcal{L}$ by 1/2 (Fig. 3). After correcting for background, our final value for g_1/f_1 is $1.32 \pm^{0.21}_{0.17\,\mathrm{stat}}$. As a check of our Monte Carlo simulation, we measure the two body asymmetry product $\alpha_\Xi \alpha_\Lambda$ with a sample of 70 000 $\Xi^0 \to \Lambda\, \pi^0$ events. We measure $\alpha_\Xi \alpha_\Lambda$ to be $-0.286 \pm 0.008_{\mathrm{stat}} \pm 0.015_{\mathrm{syst}}$ which is consistent with its value of -0.264 ± 0.013 [9].

The dominant contribution to the systematic error is due to the uncertainty in the background. Other systematic errors are estimated by changing quantities in our detector commensurate with their observed deviations from the data (Tab. I). The systematic error on g_1/f_1 due to the mass shift is found to be negligible by comparing MC simulations with Ξ^0 masses of 1.3149 GeV/c^2 and 1.3155 GeV/c^2.

Source of Uncertainty	Error on g_1/f_1
Background	0.039
Beam Shape	0.015
MC Statistics	0.020
DC Alignment	0.020
Ξ^0 Lifetime ($\pm 5\%$)	0.009
CsI Energy Scale ($\pm 0.3\%$)	0.009
Error on α_{Σ^+} ($\pm^{0.017}_{0.015}$)	0.013
Total Systematic Error	0.054

TABLE I. Systematic Error for g_1/f_1

Radiative corrections have been explicitly determined not to affect the final state polarization and electron-neutrino correlation in hyperon beta decays [10]. The standard q^2 dependence of f_1 and g_1 is used [10], neglecting the q^2 dependence of f_1 and g_1 changes the measured value for g_1/f_1 by 0.007.

If we relax the requirement that $g_2 = 0$, and fit the distributions to g_1/f_1 and g_2/f_1 simultaneously, we see no evidence for a non-zero second class current term (Fig. 4), measuring $g_1/f_1 = 1.17 \pm 0.28_{\rm stat} \pm 0.05_{\rm syst}$ and $g_2/f_1 = -1.7 \pm^{2.1}_{2.0\,\rm stat} \pm 0.5_{\rm syst}$.

Using our measured g_1/f_1, and assuming $g_2/f_1 = 0$, we then determine the value for f_2/f_1 using the electron energy spectrum in the Σ^+ frame (Fig. 2). The beta spectrum is the only kinematic quantity that depends on f_2/f_1 to lowest order in $(M_{\Xi^0} - M_{\Sigma^+})/M_{\Xi^0}$. For the f_2/f_1 measurement, we do not discard events where the magnitude of $\vec{p}_\perp$ is greater than the energy of the neutrino in the Ξ^0 frame. Using a maximum likelihood method, we find the value for f_2/f_1 is $2.0 \pm 1.2_{\rm stat} \pm 0.5_{\rm syst}$.

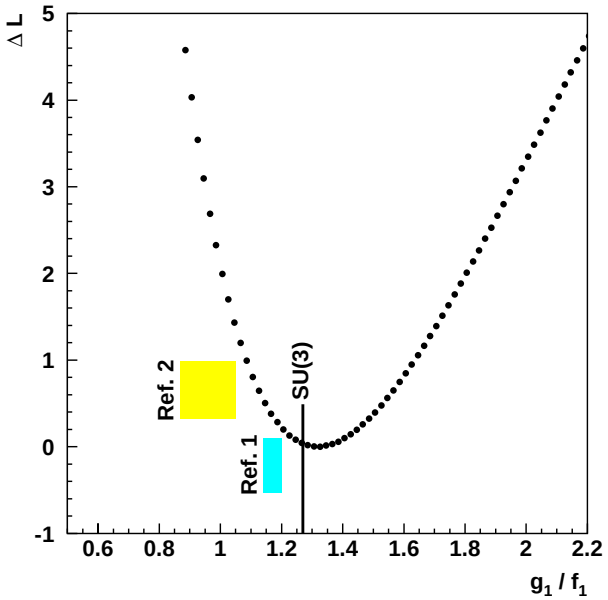

FIG. 3. Maximum likelihood fit to g_1/f_1. The shaded bands indicate the range of the theoretical predictions found in [1,2], the vertical line is the exact $SU(3)_f$ value.

The systematic errors for g_2/f_1 and f_2/f_1 are determined in a similar manner as those for g_1/f_1, however, a 0.6 MeV/c^2 shift in the Ξ^0 mass changes f_2/f_1 by 0.25, and there is also an additional error of 0.3 on f_2/f_1 due to the statistical error of g_1/f_1.

In conclusion, we have made the first measurement of g_1/f_1 for the decay $\Xi^0 \to \Sigma^+ e^- \overline{\nu}_e$, and found that $g_1/f_1 = 1.32 \pm^{0.21}_{0.17\,\rm stat} \pm 0.05_{\rm syst}$ assuming both that no second class current is present and that the weak magnetism term has the exact $SU(3)_f$ value. By using the electron-neutrino correlation and the final state polarization of the Σ^+ *via* its two body decay $\Sigma^+ \to p\,\pi^0$, we are able to determine both the sign and the magnitude of g_1/f_1. Our result agrees well with the exact $SU(3)_f$ prediction. It therefore favors $SU(3)_f$ breaking schemes that predict small corrections to g_1/f_1. Furthermore, if we relax the constraint that $g_2 = 0$, and simultaneously fit for g_1/f_1 and g_2/f_1, we see no evidence for a second class current term but the uncertainties are large. Our analysis of the electron energy spectrum in the Σ^+ frame gives a value for f_2/f_1 that is consistent with the Conserved Vector Current prediction.

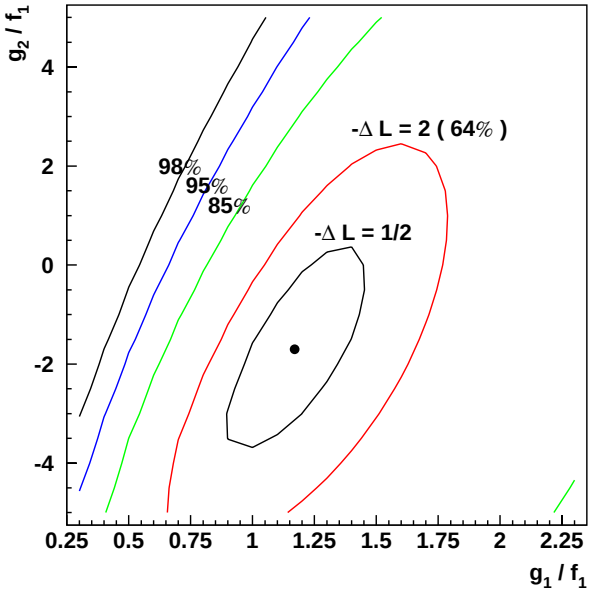

FIG. 4. Maximum likelihood fit to g_2/f_1 and g_1/f_1.

We gratefully acknowledge the support and effort of the Fermilab staff and the technical staffs of the participating institutions for their vital contributions. This work was supported in part by the U.S. Department of Energy, The National Science Foundation and The Ministry of Education and Science of Japan.

* Permanent address University of São Paulo, São Paulo, Brazil.
† Permanent address C.P.P. Marseille/C.N.R.S., France.
‡ To whom correspondence should be addressed. Electronic address: r-winston@uchicago.edu

[1] P. G. Ratcliffe, Phys. Rev. D **59**, 014038 (1999).
[2] R. Flores-Mendieta et al., Phys. Rev. D **58**, 094028 (1998).
[3] N. Cabibbo, Phys. Rev. Lett. **10**, 531 (1963).
[4] A. Affolder *et al.*, Phys. Rev. Lett. **82**, 3751 (1999). The trigger used for the present data was an improved version of the one described in this earlier paper. Further details can be found in S. Bright, Ph.D. thesis, The University of Chicago (2000).
[5] We observe that the mean Σ^+ mass is ~ 0.6 MeV/c^2 higher than its nominal value; this shift is also seen in the Ξ^0 mass from $\Xi^0 \to \Lambda\,\pi^0$ (with $\Lambda \to p\,\pi^-$) decays. Shifting the Σ^+ mass in the Monte Carlo has a negligible effect on g_1/f_1 and g_2/f_1 .
[6] J. Dworkin et al., Phys. Rev. D **41**, 780 (1990).
[7] S. Bright, R. Winston, E. C. Swallow and A. Alavi-Harati, Phys. Rev. D **60**, 117505 (1999).
[8] J. M. Watson and R. Winston, Phys. Rev. **181**, 1907 (1969).
[9] Particle Data Group, C. Caso *et al.*, Eur. Phys. J. C **3**, 1 (1998).
[10] A. Garcia and P. Kielanowski, *The Beta Decay of Hyperons*, Lecture Notes in Physics Vol. 222 (Springer-Verlag, Berlin, 1985). With these metric and γ matrix conventions, g_1/f_1 is **positive** for neutron beta decay.